Inorg. Chem. **2006**, *45*, 7210–7216

$Ce_4(P_{1-x}Si_x)_{3-z}$: A First Example for the Stabilization of the Anti-Th_3P_4 Type Structure by Substitution in the Non-Metal Substructure

Pavel S. Chizhov,*[,†,‡] Nellie R. Khasanova,[†] Michael Baitinger,[‡] Walter Schnelle,[‡] Yuri Prots,[‡] Ulrich Burkhardt,[‡] Evgeny V. Antipov,[†] and Yuri Grin[‡]

Chemistry Department, Moscow State University, 119992 Moscow, Russia, and Max-Planck-Institut für Chemische Physik fester Stoffe, Nöthnitzer Str. 40, 01187 Dresden, Germany

Received April 28, 2006

A first rare-earth phosphide silicide $Ce_4(P_{1-x}Si_x)_{3-z}$ and its analogues with La, Pr, and Nd were synthesized and characterized. The compounds crystallize in the anti-Th_3P_4 structure type. The cerium compound shows a mixed occupation of the 12*a* site with Si and P and possesses a wide homogeneity range with respect to *x* and *z* variation. The electronic configuration of Ce, deduced from magnetic susceptibility and X-ray absorption spectroscopy data, remains $4f^1$ (Ce^{3+}) independently from *x* and *z*. The cerium valence and the phase stability region are discussed employing electronic band-structure calculation and chemical bonding analysis with electron localization function. Atomic interactions are shown to remain nearly unchanged, while the change of the excess electron concentration with P/Si substitution is considered to play the main role for the stabilization of the structural motif.

Introduction

Rare-earth pnictides Ln_4Pn_3 (Ln = rare-earth metal; Pn = P, As, Sb, Bi) raised great interest after the report about heavy fermion-like behavior of Yb_4As_3.[1] This compound has an anti-Th_3P_4 type crystal structure with intermediate valence of Yb and low charge carrier concentration. The influence of the nature of pnictogen and of the rare-earth metal valence on the properties of Yb_4Pn_{3-z} has been discussed in several reports.[2−5] Similar compounds with Eu were also investigated thoroughly,[6,7] but the origin of the unusual physical properties and the homogeneity ranges for Ln_4P_3 phases are still under discussion.[8]

The isostructural compounds of lanthanides other than Yb and Eu were not investigated in detail. Most of the RE_4Pn_3 (RE = rare-earth metal with the exception of Eu and Yb) compounds are stable with heavy pnictogens (Sb, Bi).[9] Only three analogous arsenides have been described up to now (La_4As_3,[9] Ce_4As_3, and Pr_4As_3),[10] and no RE_4P_3 phosphides were found.[11] However, the higher electronegativity of phosphor might lead to a different type of chemical interaction in comparison with As and Sb. This, in turn, may result in unusual physical and structural phenomena, for example, charge ordering. Moreover, the stabilization of RE_4P_3 could provide new information about the valence state of lanthanides and chemical bonding in compounds of this type.

In the case of the phosphides RE_4P_3, assuming the oxidation state 3− of phosphor, the formal balance can be written as $(RE^{2+})_3(RE^{3+})_1(P^{3-})_3$; that is, only a part of the RE cations is required to be in the oxidation state 3+. For the RE elements with the unstable oxidation state 2+, this

* To whom correspondence should be addressed. Tel.: +4935146464209. Fax: +4935146464002. E-mail address: chizhov@cpfs.mpg.de.
† Moscow State University.
‡ Max-Planck-Institut für Chemische Physik fester Stoffe.

(1) Ochiai, A.; Suzuki, T.; Kasuya, T. *J. Phys. Soc. Jpn.* **1990**, *59*, 4129.
(2) Ochiai, A.; Aoki, H.; Suzuki, T.; Helfrich, R.; Steglich, F. *Physica B* **1997**, *230*−*232*, 708.
(3) Antonov, V. N.; Yaresko, A. N.; Perlov, A. Ya.; Thalmeier, P.; Fulde, P. *Phys. Rev. B* **1998**, *58*, 9752.
(4) Staub, U.; Shi, M.; Schulze-Briese, C.; Patterson, B. D.; Fauth, F.; Dooryhee, E.; Soderholm, L.; Cross, J. O.; Mannix, D.; Ochiai, A. *Phys. Rev. B* **2005**, *71*, 075115.
(5) Chichorek, T.; Aoki, H.; Gegenwart, P.; Lang, M.; Ochiai, A.; Steglich, F. *Physica B* **2002**, *312*−*313*, 370.
(6) Cardoso, R.; Schnelle, W.; Grin, Yu.; von Schnering, H. G. *Book of Abstracts*, VIIth European Conference on Solid State Chemistry, Madrid, Sept 15−18, 1999; Vol. I, p 117.
(7) Ochiai, A.; Shima, Y.; Shirakawa, M. *Physica B* **2002**, *312*−*313*, 362.
(8) Burkhardt, U.; Grin, Yu.; von Schnering, H. G. *Book of Abstracts*, VIth European Conference of Solid State Chemistry, Zürich, Sept 17−20, 1997; PA124.
(9) Hulliger, F.; Ott, H. R. *J. Less-Common Met.* **1977**, *55*, 103.
(10) Ono, S.; Despault, J. G.; Calvert, L. D.; Taylor, J. B. *J. Less-Common Met.* **1970**, *22*, 51.
(11) Kuz'ma, Yu.; Chykhrij, S. In *Handbook of the Physics and Chemistry of Rare Earths*; Gschneider, K. A., Jr., Eyring, L., Pecharsky, V. K., Eds.; Elsevier Science: New York, 1996; Vol. 23, Chapter 156, pp 285−427.

10.1021/ic060726h CCC: $33.50
Published on Web 08/05/2006

may be a reason that they do not form the phosphides RE_4P_3. A possible way to stabilize these compounds is a replacement of phosphor by an element of the group 14 (IVA) to provide additional sinks for electrons in the anionic part of the structure and stabilize the higher oxidation state of RE metals. The formation of such solid solutions may take place if the radii of P and of the group 14 (IVA) element are close enough and their crystal chemical behaviors are similar. These considerations point out silicon as a suitable element for replacement ($r_{cov}(Si) = 1.17$ Å, $r_{cov}(P) = 1.10$ Å).

Here, we report the first cerium phosphide silicide with the anti-Th_3P_4 type structure. Its formation proves that compounds with this type of structure can actually be stabilized by substitution in the nonmetal substructure.

Experimental Section

Preparation. Metallic cerium (99.9%, Lamprecht), crystalline silicon (99.9999%, Alfa Aesar), and red phosphorus (99.999%, Alfa Aesar) were used as initial reagents. All synthetic operations were performed in a glove box with Ar atmosphere ($p(O_2) < 0.1$ ppm, $p(H_2O) < 0.1$ ppm).

To avoid evaporation of phosphorus during the reaction, cerium monophosphide was used as a precursor for the synthesis. It was prepared by the following technique. RE metal filings and phosphorus powder were mixed in stoichiometric ratio in an agate mortar, pressed in a pellet, put in an alumina crucible, and then placed in a quartz ampule. The ampule was sealed under vacuum (10^{-4} mbar) and then annealed at 950 °C for 1 week. The heating rate was relatively low (0.6 °C/min) to allow phosphorus to react out without evaporation. The presence of single-phase CeP was confirmed by powder X-ray diffraction (PXRD) methods and energy-dispersive X-ray spectroscopy (EDXS) analysis.

In the next stage, CeP powder, Ce filings, and Si powder in the necessary ratio were ground together in an agate mortar and pressed in a pellet. The first annealing of the mixture was made under the same conditions, as described above. The sample was then thoroughly reground and pressed in a pellet before every consequent high-temperature annealing. The next two through four annealings were performed in welded Ta containers, sealed in evacuated silica ampules at 1250 °C each for 1 week. Finally, the ampules were cooled to room temperature in air.

Several samples were finally treated by arc melting in Ar atmosphere (tungsten electrode, cooled copper plate) to obtain crystals suitable for the XRD experiment.

To investigate the possible homogeneity range of $Ce_4(P_{1-x}Si_x)_{3-z}$, nine initial compositions ($x = 1/3$, 1/2, 2/3 and $z = 0$, 1/6, 1/3) were prepared. It has to be mentioned that the high stability of CeP causes kinetic troubles in the preparation of the ternary phase. Despite a long annealing time (more than 3 weeks), a CeP admixture (about 1−2 wt % from PXRD data) was found even in the best samples. All attempts to improve the quality of the educt using different methods of activation (e.g., spark plasma sintering) were not successful.

After investigation of the $Ce_4(P_{1-x}Si_x)_{3-z}$ compound several other RE−P−Si systems (RE = La, Pr, Nd, Sm, Tb, Er, Yb, Lu) were also studied for the existence of phosphide silicides with anti-Th_3P_4 crystal structure. Metallic RE metals (99.9%, Lamprecht) were used for synthesis. The preparation conditions were identical to those described for the cerium phase.

Characterization. PXRD data were collected with a Huber G670 Image Plate Guinier camera and a STOE STADI P diffractometer (Cu $K\alpha_1$ radiation, $\lambda = 1.5406$ Å, linear PSD detector). Lanthanum hexaboride ($a = 4.1569$ Å) was used as an internal standard for unit cell parameter refinement. WinCSD[12] and WinXPow[13] program packages were applied for data processing.

For metallographic investigations $\approx 2 \times 2$ mm^2 areas of the air- and water-sensitive $Ce_4(P_{1-x}Si_x)_{3-z}$ samples were prepared under inert conditions in an argon-filled glove box. The samples were embedded in two-component epoxy resin with silver filler (hardening at 100 °C for 2 h) which ensured the required electrical conductivity for scanning electron microscopy experiments. SiC paper was used for grinding, and diamond powder ($<0.25\ \mu$m) was applied for the final polishing step. A small amount of water-free hexane was added as a lubricant.

The local chemical compositions were investigated by wavelength dispersive X-ray analysis (WDXS) on a CAMECA SX100 electron microprobe with a tungsten cathode. Ce Lα, P Kα, and Si Kα lines at an electron beam excitation of 20 keV were used for determination. The spectra were recorded simultaneously on gas flow proportional counters equipped with TAP (thallium acid phthalate, $d = 12.88$ Å) and PET (pentaerythritol, $d = 4.38$ Å) monochromator crystals. Two reference compounds, Ce_5Si_4 and CeNiP, served as standards for the estimation of the Si, Ce, and P contents. The composition of each phase in a sample represents the average value of eight measurements which, in general, give an overall amount of more then 97 wt % with an accuracy of 0.15 wt % and 0.1 wt % for Ce and Si/P, respectively. Spectra up to photon energies of 25 keV recorded on a Si-drift detector of an EDXS system (EDAX) showed only the presence of the starting elements excluding a contamination of the sample and the sample surface (e.g., by oxygen).

Differential thermal analysis (DTA) was performed using a Netzsch STA 409 analyzer (thermocouple type S, sample mass 30−60 mg) in the temperature range 25−1300 °C. The samples for DTA were sealed in niobium ampules.

Crystal Structure Determination. The single crystal used for X-ray analysis was mechanically separated from the sample with initial composition $Ce_4(P_{2/3}Si_{1/3})_3$ after arc melting.

Single-crystal X-ray diffraction experiments were performed on a Rigaku AFC-7 four-circle diffraction system with Mercury 70 CCD detector (Mo Kα radiation, $\lambda = 0.7107$ Å). The absorption correction was made using the multiscan procedure. The SHELXS-97[14] program was used for structure solution, and the JANA2000[15] program package was used for structure refinement. Further experimental details are listed in Table 1, and refined atomic coordinates and displacement parameters are presented in Table 2.

To get structural information for compounds with other compositions and/or RE metals (needed for electronic structure calculations) as well as amounts of impurity phases, a Rietveld refinement procedure was implemented for several multiphase patterns. The GSAS program package[16] was used, and REP and RE_5Si_3 phases were accounted as impurities.

(12) Akselrud, L. G.; Zavalii, P. Yu.; Grin, Yu.; Pecharski, V. K.; Baumgartner, B.; Wölfel, E. *Mater. Sci. Forum* **1993**, *133*, 135.
(13) *STOE WinXPow*, version 1.2; STOE & Cie GmbH: Darmstadt, Germany, 2000.
(14) Sheldrick, G. *SHELXS-97: Program for Crystal Structure Solution*; Institüt für Anorganische Chemie der Universität Göttingen: Göttingen, Germany, 1997.
(15) Petříček, V.; Dušek, M. *JANA2000*, version 22/12/2005; Institute of Physics, Academy of Science of Czech Republic: Praha, Czech Republic, 2005.
(16) Larson, A. C.; Von Dreele, R. B. *General Structure Analysis System (GSAS)*; Los Alamos National Laboratory Report LAUR 86-748; Los Alamos National Laboratory: Los Alamos, NM, 2004.

Table 1. Crystallographic Data for $Ce_4(P_{1-x}Si_x)_{3-z}$, $x = 0.41$ and $z = 0$

composition	$Ce_4(P_{0.59}Si_{0.41})_3$
space group	$I\bar{4}3d$ (No. 220)
a	8.9359(2) Å
V	713.53(5) Å^3
Z	4
ρ_{calcd}	6.047 g/cm^3
T	22 °C
crystal size	0.2 mm × 0.2 mm × 0.2 mm
color	black, metallic luster
wavelength	Mo Kα; 0.7107 Å
2θ range	6.4−65.4°
total number of reflections	3154
number of independent reflections	229
number of observed reflections ($I_{obs} > 3\sigma(I_{obs})$)	224
weighting scheme	$1/\sigma^2$
number of refined parameters	7
extinction coefficient	0.0019(2)
R_{int}	0.020
R_1[a]	0.017
wR_2[b]	0.056
largest diff. peak	0.95 e$^-$/Å^3

[a] $R_1 = [\sum||F_{obs}| - |F_{calcd}||]/\sum|F_{obs}|$. [b] $wR_2 = \{[\sum w[(F_{obs})^2 - (F_{calcd})^2]^2]/[\sum w(F_{obs}^2)^2]\}^{1/2}$.

Table 2. Atomic Coordinates and Displacement Parameters (Å^2) for $Ce_4(P_{1-x}Si_x)_{3-z}$, $x = 0.41$ and $z = 0$

atom	site	x	y	z
Ce	16*c*	0.06695(2)	x	x
$P_{0.59}Si_{0.41}$	12*a*	3/8	0	1/4

atom	U_{11}	U_{22}	U_{33}	U_{12}	U_{13}	U_{23}	U_{eq}
Ce	0.0110(1)	U_{11}	U_{11}	−0.0008(1)	$-U_{12}$	$-U_{12}$	0.0110(1)
$P_{0.59}Si_{0.41}$	0.0096(5)	U_{11}	0.0134(9)	0	0	0	0.0108(4)

Magnetic Susceptibility Measurements. Magnetic susceptibility measurements were made using a Quantum Design MPMS XL-7 SQUID magnetometer. The temperature dependence of the magnetic susceptibility was measured in different external fields (100 Oe, 1 kOe, 10 kOe) in the temperature range of 1.8−400 K.

X-ray Absorption Spectroscopy (XAS) Measurements. XAS measurements on the Ce L_{III} edge were performed at the EXAFS II beam-line E4 of HASYLAB at DESY (Hamburg, Germany). During the measurements, $Ce_4(P_{1-x}Si_x)_{3-z}$ samples, ground together with dry B_4C powder, were encapsulated in vacuum-tight stainless steel containers, equipped with beryllium windows of 0.5 mm thickness. These containers were sealed with indium wire.

Wavelength selection was realized by means of a double-crystal Si(111) monochromator with digitally stabilized components. Essential detuning for the suppressing of second harmonics was applied. The obtained resolution was about 1 eV at the Ce L_{III} edge. Measurements were made simultaneously with CeO_2 as the reference compound.

Calculation Procedure. The TB-LMTO-ASA program package[17] with LDA exchange correlation potential according to Barth and Hedin[18] was used for quantum chemical calculations. The calculations were performed for $Ce_4(P_{2/3}Si_{1/3})_3$, $Ce_4(P_{1/2}Si_{1/2})_3$, and $Ce_4(P_{1/3}Si_{2/3})_3$ compositions with ordered models, where the arbitrary, but fixed distribution of P and Si inside the conventional unit cell was taken. This assumption, in turn, led to the reduction of symmetry (space group $P1$ was used).

Table 3. Atomic Spheres Radii, Applied for TB-LMTO-ASA Calculations

$Ce_4(P_{1-x}Si_x)_{3-z}$		Ce_4P_3		Ce_4Si_3		$La_4(P_{1-x}Si_x)_{3-z}$	
atom	r (Å)	atom	r (Å)	atom	r (Å)	atom	r (Å)
Ce	1.839−1.855	Ce	1.831	Ce	1.832	La	1.872−1.908
P	1.564	P	1.514	Si	1.544	P	1.560
Si	1.579	E1	0.951	E1	0.974	Si	1.595
E	0.747−1.048	E2	0.740	E2	0.754	E	0.761−1.054

For comparison with the ternary compounds, electronic band structures of the hypothetical binary compounds Ce_4P_3 and Ce_4Si_3 were calculated. The unit cell parameters ($a = 8.9262$ Å for Ce_4P_3 and $a = 9.0025$ Å for Ce_4Si_3) with Ce coordinates (x,x,x; $x = 0.0666$ for Ce_4P_3 and $x = 0.0670$ for Ce_4Si_3) were deduced by extrapolation of the corresponding experimental parameters of $Ce_4(P_{1-x}Si_x)_{3-z}$ to $x = 0$, $z = 0$ and $x = 1$, $z = 0$, respectively.

Well-known problems with the LDA-based treatment of highly localized states (Ce(4f)) were the reason to perform also the electronic structure calculation for $La_4(P_{1/2}Si_{1/2})_3$ ($a = 9.0980$ Å, x(La) = 0.0661), where 4f orbitals of the RE are unoccupied. The distribution of P and Si was the same as in the case of $Ce_4(P_{1/2}Si_{1/2})_3$.

The calculations were made for 8 k points in the irreducible Brillouin zone (IBZ) in the case of ordered low-symmetrical $Ce_4(P_{1-x}Si_x)_{3-z}$ and $La_4(P_{1/2}Si_{1/2})_3$ compounds and for 10 k points in the IBZ in the case of Ce_4P_3 and Ce_4Si_3. Integration over the Brillouin zone was made by the tetrahedron method, with 24 or 30 inequivalent tetrahedrons in the IBZ, for $Ce_4(P_{1-x}Si_x)_{3-z}/La_4(P_{0.5}Si_{0.5})_3$ and for Ce_4P_3/Ce_4Si_3, respectively.

The radial scalar-relativistic Dirac equation was solved to get the partial waves. Although the calculation within the atomic sphere approximation (ASA) includes corrections for the neglect of interstitial regions and partial waves of higher order,[19] an addition of empty spheres in the cases of all the compounds was necessary. The radii of the atomic spheres, applied for calculation, are listed in Table 3.

A basis set containing Ce(6s,5d,4f) or La(6s,5d,4f), P(3s,3p), and Si(3s,3p) orbitals was employed for the self-consistent calculation with the Ce(6p) or La(6p), the P(3d) and Si(3d) functions being downfolded.

The electron localization function (ELF, η) was evaluated according to ref 20 with an ELF module already implemented within the TB-LMTO-ASA program package.[17] To gain a deeper insight into the chemical bonding, the topology of ELF was analyzed with the program Basin.[21] The electron density was integrated in basins, which are bounded by zero-flux surfaces in the gradient of ELF. This method, analogous to the procedure proposed by Bader for the electron density,[22]resulted for each basin in an electron count, revealing basic information for the description of the bonding situation.

Results and Discussion

Homogeneity Range of $Ce_4(P_{1-x}Si_x)_{3-z}$. The new cubic phase with $a \approx 9$ Å was found in all prepared samples. Lattice parameter values, observed extinctions, and diffraction intensities distribution indicated the formation of an anti-

(17) Jepsen, O.; Burkhardt, A.; Andersen, O. K. *The TB-LMTO-ASA Program*, version 4.7; Max-Planck-Institut für Festkörperforschung: Stuttgart, Germany, 1999.
(18) Barth, U.; Hedin, L. *J. Phys. C* **1972**, *5*, 1629.
(19) Andersen, O. K. *Phys. Rev. B*, **1975**, *12*, 3060.
(20) Savin, A.; Flad, H. J.; Preuss, H.; von Schnering, H. G. *Angew. Chem.* **1992**, *104*, 185; *Angew. Chem., Int. Ed. Engl.* **1992**, *31*, 185.
(21) Kohout, M. *BASIN*, version 2.3; Max-Planck-Institut für Chemische Physik fester Stoffe: Dresden, Germany, 2001.
(22) Bader, R. F. W. *Atoms in molecules: a quantum theory*; Oxford University Press: Oxford, 1999.

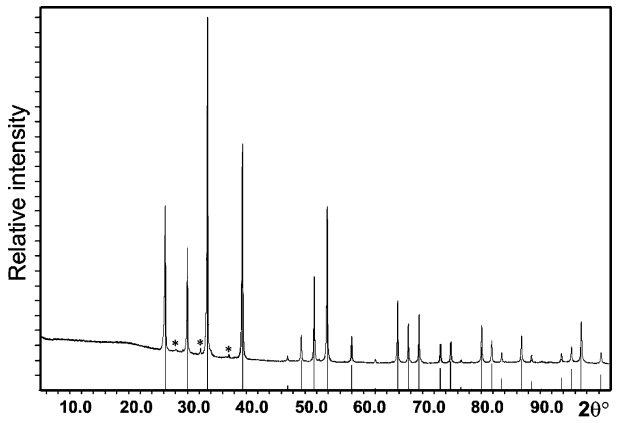

Figure 1. PXRD pattern of the $Ce_4(P_{0.5}Si_{0.5})_3$ sample. Impurity peaks (CeP) are marked by asterisks.

Table 4. Unit Cell Parameters of the $Ce_4(P_{1-x}Si_x)_{3-z}$ Phase for Different Compositions

composition (normalized to $Ce_4P_aSi_b$)				
initial mixture	WDXS	x	z	a (Å)
$Ce_4P_{1.78}Si_{0.89}$	$Ce_{4.000(3)}P_{1.80(2)}Si_{0.86(2)}$	0.32(1)	0.34(3)	8.9299(2)
$Ce_4P_{1.89}Si_{0.94}$	$Ce_{4.000(8)}P_{1.82(2)}Si_{0.97(1)}$	0.35(1)	0.21(3)	8.9282(1)
$Ce_4P_{2.00}Si_{1.00}$[a]	$Ce_{4.000(7)}P_{1.44(1)}Si_{1.51(2)}$	0.51(1)	0.06(3)	8.9776(4)
$Ce_4P_{1.50}Si_{1.50}$	$Ce_{4.000(7)}P_{1.37(2)}Si_{1.59(2)}$	0.54(1)	0.04(3)	8.9966(2)
$Ce_4P_{1.42}Si_{1.42}$	$Ce_{4.000(7)}P_{1.25(2)}Si_{1.51(3)}$	0.55(2)	0.24(5)	8.9997(2)
$Ce_4P_{1.33}Si_{1.33}$	$Ce_{4.000(7)}P_{1.21(2)}Si_{1.46(2)}$	0.55(2)	0.34(4)	8.9801(5)
$Ce_4P_{0.94}Si_{1.89}$[b]	$Ce_{4.000(7)}P_{1.30(1)}Si_{1.67(2)}$	0.56(1)	0.01(3)	9.0107(2)

[a] About 35% (by mass) of the CeP admixture. [c] About 20% (by mass) of the Ce_5Si_3 admixture.

Th_3P_4 type of the crystal structure (space group $I\bar{4}3d$). A PXRD pattern of $Ce_4(P_{0.5}Si_{0.5})_3$ is shown in Figure 1.

The lattice parameter a varied for different samples, suggesting the existence of a homogeneity range of cerium phosphide silicide. WDXS investigation confirmed this suggestion and allowed the x and z values to be related to the lattice parameter (Table 4).

For most samples the composition, observed from WDXS, is close to the one of the initial mixture. Certain differences in several cases are mainly caused by the presence of impurities, especially of CeP. The stability of the monophosphide leads to a reduced P content in the ternary compound respective to the initial composition. The Si-rich boundary concentration was found at $x \approx 0.56$. The z value changes from 0.01(3) to 0.34(3), which is very close to the range of 0−1/3 in initial mixtures. Analysis of the literature data for anti-Th_3P_4 type phases did not reveal representatives with defects concentration on the 12*a* position larger than 1/3.

The lattice parameter changes monotonically in the range of 9.0107(2)−8.9282(2) Å, increasing with increasing x and/or decreasing z. The dependence $a(x,z)$ was approximated by a bilinear function $a = 8.7401 + 0.4783x + 0.3292z - 0.6877xz$; the obtained surface and experimental points are shown in Figure 2.

The DTA measurements for selected samples $Ce_4(P_{1-x}Si_x)_{3-z}$ (x = 1/3, 1/2, 2/3; z = 0) did not reveal decomposition, melting, or any phase transition up to 1300 °C.

$RE_4(P_{1-x}Si_x)_{3-z}$ Phases. The $RE_4(P_{1-x}Si_x)_{3-z}$ compounds form only for the light lanthanides La, Pr, and Nd, similar

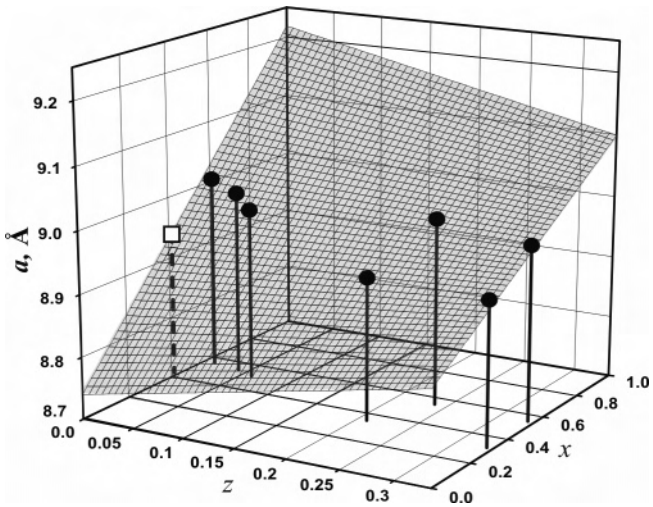

Figure 2. Lattice parameter a vs composition (x,z) for $Ce_4(P_{1-x}Si_x)_{3-z}$. The calculated $a(x,z)$ values are shown as a plane, and experimental points are depicted (filled circles). The determined composition for the single crystal is shown by the open square.

Table 5. Composition of Initial Mixtures and Unit Cell Parameters for $RE_4(P_{1-x}Si_x)_{3-z}$ (RE = La, Pr, Nd)

sample	a, Å	V, Å^3
$La_4(P_{0.5}Si_{0.5})_{2.83}$	9.0980(8)	753.07
$Pr_4(P_{0.5}Si_{0.5})_{2.66}$	8.8998(3)	704.92
$Nd_4(P_{0.5}Si_{0.5})_{2.66}$	8.8701(2)	697.89

to the RE−As systems.[9,10] The unit cell parameters vary in the range of 9.0980(8)−8.8701(2) Å and decrease from La to Nd (see Table 5). Preliminary results showed that the compounds also have a certain homogeneity range.

Crystal Structure. In the crystal structure of $Ce_4(P_{1-x}Si_x)_{3-z}$ both silicon and phosphorus occupy the 12*a* position. Attempts to refine the Si/P ratio led to rather unstable results because of the similar scattering power of the elements. The lattice parameter, obtained from single-crystal PXRD data (8.9485(7) Å), was close to the parameter found for the initial $Ce_4(P_{2/3}Si_{1/3})_3$ bulk sample from PXRD data (8.9359(2) Å before and 8.938(2) Å after arc melting). The lattice parameter (8.9359(2) Å) determined from the standardized PXRD was used for further calculations. Implying the obtained $a(x,z)$ dependence, it was possible to determine $x = 0.41$ (see Figure 2), assuming $z = 0$ (as it was clearly seen by the refinement of the 12*a* position). The resulting occupancies (0.59 for P and 0.41 for Si) were fixed during the refinement. The refinement of the occupancy of the Ce position gives the value 1.00(1), so this parameter was also fixed during the final refinement steps. Thus, the corresponding composition is $Ce_4(P_{0.59}Si_{0.41})_3$.

The crystal structure of $Ce_4(P_{0.59}Si_{0.41})_3$ belongs to the anti-Th_3P_4 type. The coordination polyhedra of Ce and Si/P atoms are shown in Figure 3. $Ce(P,Si)_6$ is a distorted octahedron with three short (2.9409(2) Å) and three long (3.2574(2) Å) contacts. In addition, each cerium has also five Ce neighbors: three at the distance of 3.4833(3) Å and two at 3.8694(3) Å. $Ce(P,Si)_6$ octahedra are typical building blocks for cerium silicides (e.g., Ce_5Si_3)[23] and phosphides (CeP).[24] The $Ce(P,Si)_6$ octahedra in the crystal structure of $Ce_4(P_{1-x}Si_x)_{3-z}$ are condensed via opposite faces, forming

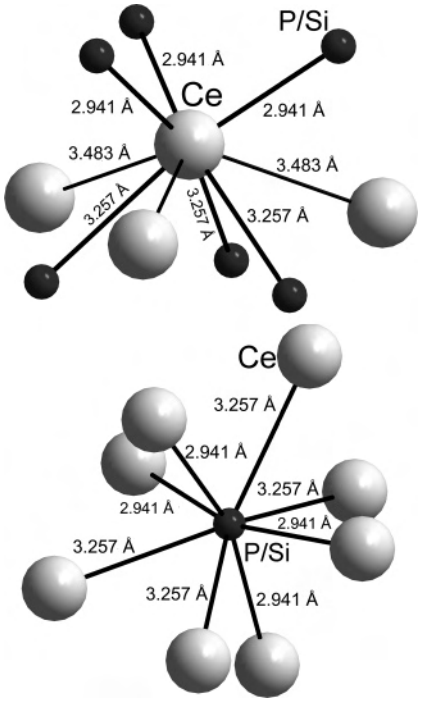

Figure 3. Coordination polyhedra of Ce and P,Si in $Ce_4(P_{1-x}Si_x)_{3-z}$, $x = 0.41$ and $z = 0$.

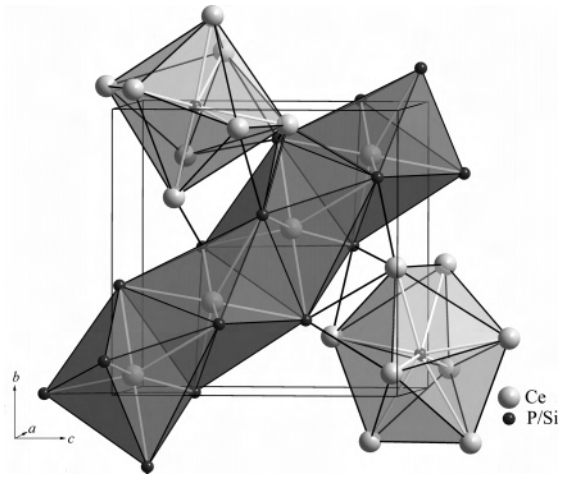

Figure 4. Arrangement of the $Ce(P,Si)_6$ and $(P,Si)Ce_8$ polyhedra in the structure of $Ce_4(P_{1-x}Si_x)_{3-z}$. Several atoms and bonds are not shown for simplicity.

columns running along the body diagonals of the cubic cell (Figure 4) and interlinked via side edges and faces. The average cerium−nonmetal distance in the octahedra (3.0992 Å) lies between the corresponding values for Ce_5Si_3 (3.227 Å, for Ce1 in the 4*c* position) and CeP (2.973 Å). The distortion of the $Ce(P,Si)_6$ octahedra in the cerium phosphide silicide, compared with the binary compounds, might suggest some kind of ordering of Si and P in the anionic substructure with a corresponding distortion of the metal substructure. This phenomenon would result in the symmetry reduction and/or the occurrence of a superstructure in the diffraction

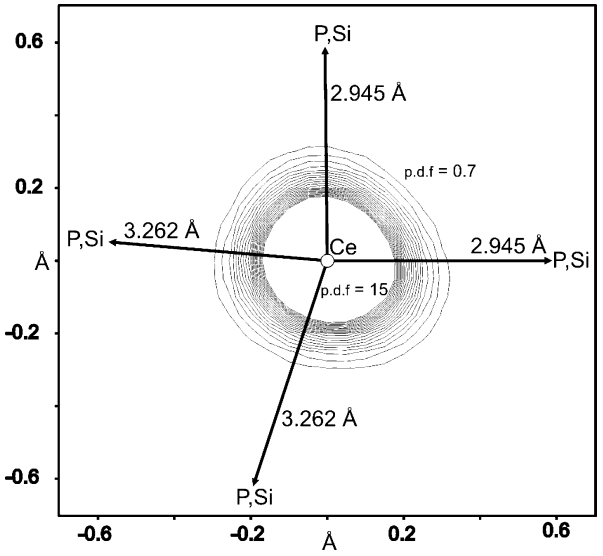

Figure 5. Probability density function (p.d.f.) of Ce in the (P,Si)−Ce−(P,Si) plane. Ce−(P,Si) bond directions are marked.

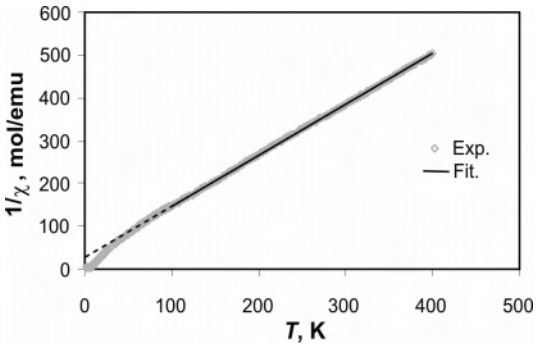

Figure 6. Inverse magnetic susceptibility $1/\chi$ vs temperature T ($H = 10$ kOe) for $Ce_4(P_{1/2}Si_{1/2})_{2.83}$.

pattern. However, no evidence for superstructure (or symmetry reduction) was found, neither from powder nor from single-crystal XRD investigations. In addition, the ordering of silicon and phosphorus should result in a detectable distortion of the spherical probability density function (p.d.f.) for Ce. To prove this possibility, the refinement of Ce ADPs as a third rank tensor was performed. The obtained p.d.f. for Ce in the (P,Si)−Ce−(P,Si) plane is shown in Figure 5. It is clearly seen that the deviation from a spherical distribution is negligible and does not reveal any preferable direction.

Magnetic Properties of $Ce_4(P_{1-x}Si_x)_{3-z}$. The magnetic susceptibility data $\chi(T,H)$ of samples which contained larger amounts of impurities were corrected. The amount of CeP, the only significant impurity, was determined from the WDXS and Rietveld refinement data. CeP is paramagnetic with known Curie−Weiss parameters ($C_{CeP} = 0.79$ mol/emu, $\Theta_{CeP} = +10$ K).[25,26] After eventual correction, the data $\chi(T)$ reveal the typical crystal field susceptibility for the $^2F_{5/2}$ ground multiplet of cerium in the $4f^1$ configuration (Ce^{3+}). At high temperatures (100−400 K) an approximate effective magnetic moment can be extracted from a linear fit to $1/\chi(T)$ (Figure 6). The obtained parameters are listed in Table 6. Obviously, the electronic configuration of Ce is $4f^1$ (for comparison: $\mu_{free} = 2.54\ \mu_B$) in all studied samples and is

(23) Gladyshevskii, E. I.; Kripyakevich, P. I. *Inorg. Mater. (USSR)* **1965**, *1*, 644.
(24) Ono, S.; Nomura, K.; Hayakawa. H. *J. Less-Common Met.* **1974**, *38*, 119.

Table 6. Magnetic Properties of $Ce_4(P_{1-x}Si_x)_{3-z}$ Samples

sample composition (initial mixture)	impurity (mass %; PXRD data)	effective magnetic moment per Ce atom (μ_B), $H = 10$ kOe	Weiss parameter θ (K), $H = 10$ kOe
$Ce_4(P_{1/2}Si_{1/2})_{2.83}$	~1% of CeP	2.60	−25
$Ce_4(P_{1/2}Si_{1/2})_3$	12% CeP[a]	2.60	−24
$Ce_4(P_{2/3}Si_{1/3})_3$	20% CeP[a]	2.58	−27
$Ce_4(P_{1/3}Si_{2/3})_3$	2−3% of unknown impurity	2.61	−29

[a] Rietveld refinement data.

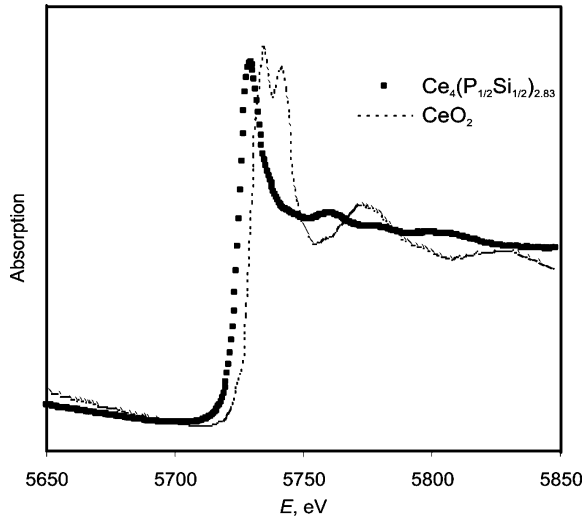

Figure 7. XAS spectrum of $Ce_4(P_{1/2}Si_{1/2})_{2.83}$ compared with CeO_2.

not significantly influenced by the Si/P ratio. At low fields ($H = 100$ K) a splitting of zero-field cooled and field cooled data of $\chi(T)$ is observed at temperatures of 2.7−3.5 K hinting for a magnetic transition. The character of this transition is neither clearly antiferro- nor ferromagnetic and might be spin-glass-like. The reason for the glass-like transition could be the random occupation (disorder of Si and P) on the Si/P site.

Ce L_{III} XAS Spectra. The existence of only one narrow absorption maximum lying 5 eV lower than the first white line of the CeO_2 standard clearly evidences the $4f^15d^0$ electron configuration of Ce in $Ce(P_{1/2}Si_{1/2})_{2.83}$ (Figure 7). The spectra of other $Ce_4(P_{1-x}Si_x)_{3-z}$ samples are not significantly influenced by the variation of x and z, which fully coincides with magnetic susceptibility data. Two weak shoulders on the high-energy side of the main absorption peak are probably caused by a CeP impurity (according to refs 25−27, part of Ce in CeP exists in the $4f^05d^0$ state).

Electronic Structure and Chemical Bonding. The calculated electronic band structures of $Ce_4(P_{1-x}Si_x)_3$ for x values of 1/3, 1/2, and 2/3 are very similar and can be described within a rigid-band scheme. Thus, only the calculated density of states (DOS) and partial DOS for $Ce_4(P_{1/2}Si_{1/2})_3$ are presented in Figure 8 in comparison with those of $La_4(P_{1/2}Si_{1/2})_3$.

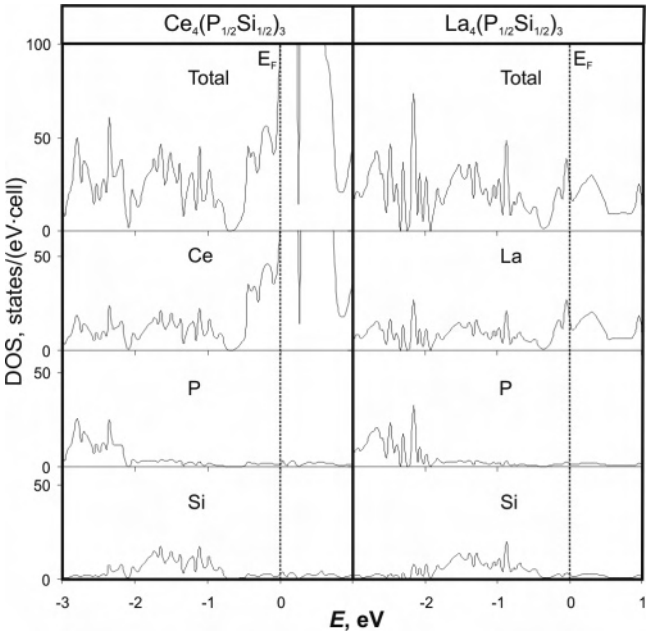

Figure 8. Electronic total and partial DOS for $Ce_4(P_{2/3}Si_{1/3})_3$ and $La_4(P_{2/3}Si_{1/3})_3$.

The similarity of the electronic structures of Ce and La-based compounds is obvious. The only difference is caused by localized Ce(4f) states, which are not sufficiently described in a LDA approach.

The valence band is located at $E < -0.5$ eV (respective to E_F) and can be considered as consisting of two parts. At $E < -2$ eV the contribution of the phosphorus s and p states prevail, very similar to the hypothetical binary Ce_4P_3 compound. In the region -2 eV $< E < -0.5$ eV the s and p states of silicon dominate, in good agreement with the DOS for hypothetical Ce_4Si_3. In both parts a RE metal contributes mainly with s states and small amounts of d states. The valence band is separated from the conduction band by a (pseudo)gap of ≈0.5 eV. This kind of DOS topology is in accordance with the formation of isolated P and Si anions. The main contribution to the DOS at the Fermi level is made by RE (4f,5d) states, both in Ce- and La-based $RE_4(P_{1-x}Si_x)_3$ compounds.

Taking these results together with chemical composition (Table 4), magnetic susceptibility, and XAS data, we propose a simple Zintl-like scheme for the description of the electronic structure of $RE_4(P_{1-x}Si_x)_{3-z}$ compounds. Therein, the formal charge balance for these compounds is written as $(RE^{3+})_4(P^{3-}_{1-x}Si^{4-}_x)_{3-z}\cdot(3 - 3x + 3z + xz)e^-$. The electron configuration of the RE cation remains unchanged with the P/Si substitution (i.e., $4f^15d^06s^0$ for Ce^{3+} and $4f^05d^06s^0$ for La^{3+}) as concluded from magnetic susceptibility and XAS data. The amount of excess electrons varies in the range of 1.4−3.1 e^- per f.u. (0.12−0.26 e^- per each cation charge unit), using the composition as revealed by WDXS (Table 4). These values are to be treated semiquantitatively, as several approximations (full charge transfer, conservation of the electronic structure with the vacancies formation) were used. However, it seems reasonable to conclude the existence of the narrow range of the excess electron concentration, where the $Ce_4(P_{3-x}Si_x)_{3-z}$ compound is stable.

(25) Hulliger, F.; Ott, H. R. *Z. Physik B* **1978**, *29*, 47.
(26) Rossat-Mignod, J.; Burlet, P.; Quezel, S.; Effantin, J. M.; Delacote, D.; Bartholin, H.; Vogt, O.; Ravot, D. *J. Magn. Magn. Mater.* **1983**, *31−34*, 398.
(27) Laegsgaard, J.; Svane, A. *Phys. Rev. B* **1998**, *58*, 12817.

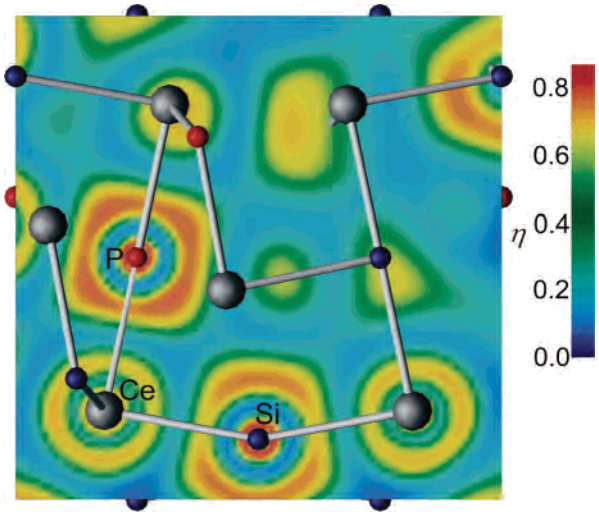

Figure 9. ELF distribution in the P−Ce−Si plane for $Ce_4(P_{1/2}Si_{1/2})_3$.

It is worthwhile to emphasize an unusual relationship with the bonding situation in $Mg_{1-x}B_2$ and $Al_{1-x}B_2$ compounds, where nearly the same excess electron concentration is needed for the stabilization of the structure (0.23 e^- per cation charge).[28,29]

Comparing the amount of excess electrons for the compound with different compositions, one might note that maximal calculated value for the real compound (3.1 e^- per f.u.) exceeds one for the hypothetical Ce_4P_3 (3.0 e^- per f.u.). However, the calculated lattice parameter for Ce_4P_3 ($x = 0$, $z = 0$ in $Ce_4(P_{1-x}Si_x)_{3-z}$) is rather small (8.7401 Å), suggesting the existence of smaller Ce^{4+} cations in the anti-Th_3P_4 type phosphide. It would lead to the increase of the amount of excess electrons and, consequently, to the instability of the structure. Moreover, no evidence of the Ce^{4+} presence in the anti-Th_3P_4 type phosphide silicides was found from the experimental studies (see magnetic properties and XAS data).

Further insight was obtained from the investigation of the chemical bonding with the ELF. ELF belongs to the so-called bonding indicators in real space[30] and represents, in a general sense, a charge distribution of electron pairs,[31] which play the main role in chemical bonding according to the Lewis theory. ELF in the vicinity of the nuclei reveals the closed-shell situation in the inner shells, and the integrated electronic density values inside the corresponding shell basins (electron counts) are in a good agreement with values, expected from the Aufbau principle.[32] The ELF maxima in the valence region indicate directed (covalent) bonding, while the integration of the electron density in the corresponding basins provides the electron count for each bond.

In $La_4(P_{1-x}Si_x)_{3-z}$ (and in $Ce_4(P_{1-x}Si_x)_{3-z}$) the spatial distribution of the ELF has a pronounced shell-like character. All shell basins (five for La and three for Si and P) are centered by nuclei (Figure 9). No additional attractors were found between the atoms. These features fit well the closed-shell picture and suggest strongly polar (ionic) character of the interactions between RE atoms and Si/P. The integration of the electron density in the shell basins gives the formal charges of −2.52 for P and −3.30 for Si in $La_4(P_{1/2}Si_{1/2})_3$. This is definitely smaller than expected from the Zintl model (−3 for P and −4 for Si). Relatively small anion charges are related to the partial charge transfer for RE: La has the charge +2.09 in $La_4(P_{1/2}Si_{1/2})_3$); that is, in the ELF representation the electrons of the fifth shell (5d) of RE atoms do not participate in the bonding interaction in the valence region. A similar behavior was found for lanthanum atoms in $La_{16}Al_{13}$, where the formal charge of +2 was obtained for lanthanum from combined ELF/electron density calculations.[33]

Conclusions

The first RE phosphide silicide $Ce_4(P_{1-x}Si_x)_{3-z}$ with anti-Th_3P_4 type of crystal structure exists in a wide homogeneity range. The electronic configuration of Ce (deduced from magnetic susceptibility data and XAS) remains invariable ($4f^1$) with x/z variations. Strongly polar (ionic) interactions between anionic and cationic substructures, invariable with P/Si substitution, were observed for $RE_4(P_{1-x}Si_x)_{3-z}$ compounds. It points out the excess electron concentration change as the possible reason for structure stabilization; that is, the structure becomes unstable both at the high and the low amounts of the excess electrons.

Acknowledgment. The authors thank M. Eckert and K. Schulze for metallographic investigations and WDXS measurements, R. Koban for magnetic susceptibility measurements, Dr. S. Budnyk and Dr. M. Schmidt for XAS measurements, Prof. Dr. R. Niewa and S. Müller for DTA measurements, and N. Reinfried and F. Thoss for performing the spark plasma sintering preparations. This work was partly supported by RFBR (Project No. 06-03-33066).

Supporting Information Available: Crystallographic data in CIF format. This material is available free of charge via the Internet at http://pubs.acs.org.

IC060726H

(28) Schmidt, J.; Schnelle, W.; Grin, Yu.; Kniep, R. *Solid State Sci.* **2003**, *5*, 535−539.
(29) Burkhardt, U.; Gurin, V.; Haarmann, F.; Borrmann, H.; Schnelle, W.; Yaresko, A.; Grin, Y. *J. Solid State Chem.* **2004**, *177*, 389−394.
(30) Kohout, M.; Pernal, K.; Wagner, F. R.; Grin, Yu. *Theor. Chem. Acc.* **2004**, *112*, 453.
(31) Kohout, M. *Int. J. Quantum Chem.* **2004**, *97*, 651.
(32) Kohout, M.; Savin, A. *Int. J. Quantum Chem.* **1996**, *60*, 875.
(33) Niewa, R.; Kirchner, M.; Zhang, H.; Schnelle, W.; Grin, Yu. *Z. Kristallogr.* **2005**, *220*, 115.